

Supporting Information

Characterization of the Dynamics in the Protonic Conductor CsH₂PO₄ by ¹⁷O Solid-State NMR Spectroscopy and First-Principles Calculations: Correlating Phosphate and Protonic Motion

Gunwoo Kim,¹ John M. Griffin,¹ Frédéric Blanc,^{1,#}

Sossina M. Haile,² and Clare P. Grey^{1,3}*

¹ Department of Chemistry, University of Cambridge,

Lensfield Road, Cambridge, CB2 1EW, United Kingdom,

² Materials Science, California Institute of Technology, 1200 E. California Boulevard,

Pasadena, CA 91125, USA.

³ Department of Chemistry, Stony Brook University,

Stony Brook, NY 11790-3400, United States.

Present address: [#] Department of Chemistry, University of Liverpool,

Stephenson Institute for Renewable Energy, Liverpool, L69 7ZD, United Kingdom,

* Author to whom correspondence should be addressed (C.P.G.):

Email: cpg27@cam.ac.uk; Phone: +44 (0)1223 336509; Fax: +44 (0)1223 336509.

Table of Contents

- 1. Summary of hydrogen bond configurations in paraelectric CsH₂PO₄ as determined by single crystal neutron diffraction (Table S1)**
- 2. Powder X-ray diffraction (Figure S1)**
- 3. Simulated 1D spectra with and without ¹⁷O CSAs (Figure S2 and Table S2)**
- 4. Room-temperature ¹⁷O MAS NMR spectra obtained at different magnetic fields (Figure S3)**
- 5. Possible local hydrogen-bonding arrangements and their calculated NMR parameters (Figure S4 and Table S3)**
- 6. Simulated 1D spectra as a function of a hopping frequency (Figure S5)**
- 7. 2D ¹⁷O MQMAS spectrum (Figure S6)**
- 8. ¹H-¹⁷O heteronuclear correlation (HETCOR) spectrum (Figure S7)**
- 9. Variable-temperature ¹⁷O MAS spectra with full spectral width (Figure S8)**
- 10. Room-temperature ¹⁷O MAS NMR spectra with and without ¹H decoupling (Figure S9)**
- 11. Tables showing the correlations between the rates of phosphate rotation and proton hop rates (Table S4 and S5)**

1. Summary of hydrogen bond configurations in paraelectric CsH₂PO₄ as determined by single crystal neutron diffraction

Table S1. Hydrogen bond configurations in paraelectric CsH₂PO₄ as determined by single crystal neutron diffraction by Nelmes and Choudhary.¹ Number in parentheses indicates uncertainty in the final digit. Some authors place the H2 atom in a fully occupied position centered between O3 atoms.

Hydrogen bond	$d(\text{O}^{\text{d}} \dots \text{O}^{\text{a}})$ (Å)	$d(\text{O}^{\text{d}}\text{-H})$ (Å)	$d(\text{O}^{\text{a}} \dots \text{H})$ (Å)	$\angle\text{OHO}$ (°)
O1–H1⋯O2	2.521(7)	0.997(7)	1.530(7)	173.2(5)
O3⋯H2 _{1/2} H2 _{1/2} ⋯O3	2.46(1)	1.00(2)	1.46(2)	174(4)

2. Powder X-ray diffraction (PXRD).

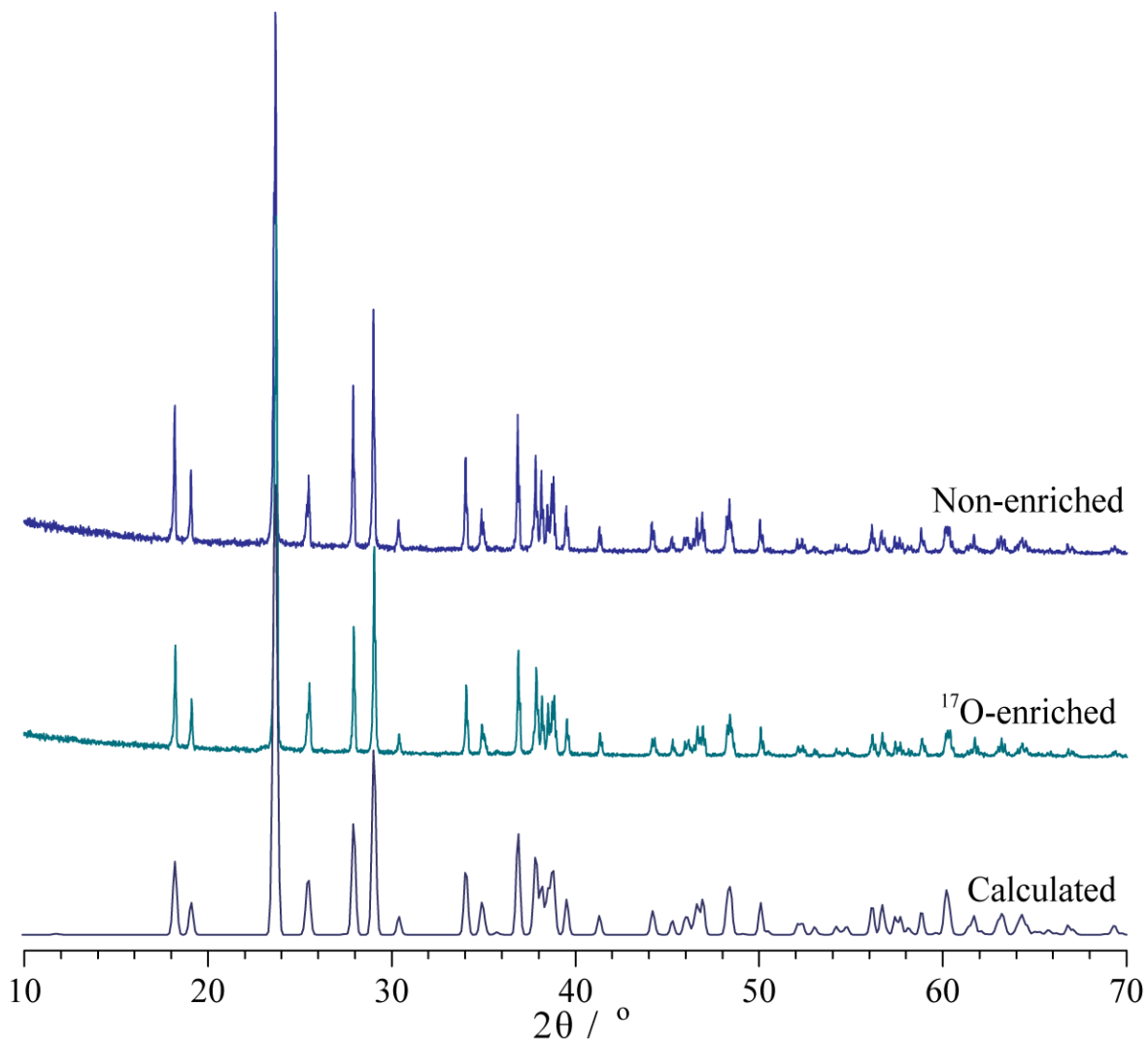


Figure S1. PXRD patterns of all non-¹⁷O-enriched CsH₂PO₄ samples, showing the monoclinic phase (space group P2₁/m) at room temperature. The corresponding calculated pattern from the ICSD (no. 79608²) is shown for comparison.

3. Simulated 1D spectra with and without the ^{17}O CSAs (Figure S2 and Table S2)

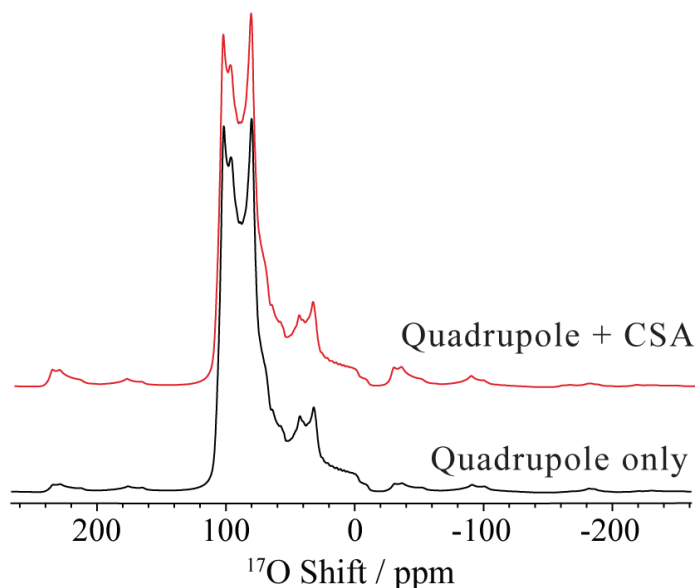


Figure S2. Simulated ^{17}O NMR spectra of CsH_2PO_4 with and without the ^{17}O CSAs, using the EXPRESS program package. It indicates that the effect of ^{17}O CSA on the lineshape is negligible (not detectable) in our simulations.

Table S2. Calculated ^{17}O CSA NMR parameters for CsH_2PO_4 using the off-centered H-bonding configuration as shown in Figure 1c.

site	$\delta_{\text{iso}}^{\text{calc}} / \text{ppm}$	$\delta_{\text{aniso}}^{\text{calc}} / \text{ppm}^{[\text{a}]}$	η^{calc}	
O1	78.1	83.2	0.11	
O3 ^d -H2...O3 ^a	O2	110.0	64.9	0.27
	O3 ^d	103.0	78.3	0.15
O3 ^a	125.7	57.5	0.51	

^[a] Reduced anisotropy defined by Haeberlen-Mehring-Spiess convention; $\delta_{\text{iso}} = \frac{\delta_{11} + \delta_{22} + \delta_{33}}{3}$, $\delta_{\text{aniso}} = \delta_{33} - \delta_{\text{iso}}$, $\eta = \frac{\delta_{22} - \delta_{11}}{\delta_{\text{aniso}}}$ where δ_{11} , δ_{22} , and δ_{33} are the principal components of the shift tensors in the order of $\delta_{11} \geq \delta_{22} \geq \delta_{33}$ (*i.e.*, $\approx \sigma_{33} \geq \sigma_{22} \geq \sigma_{11}$) and $|\delta_{33} - \delta_{\text{iso}}| \geq |\delta_{11} - \delta_{\text{iso}}| \geq |\delta_{22} - \delta_{\text{iso}}|$.

4. Room-temperature ^{17}O MAS NMR spectra obtained at different magnetic fields.

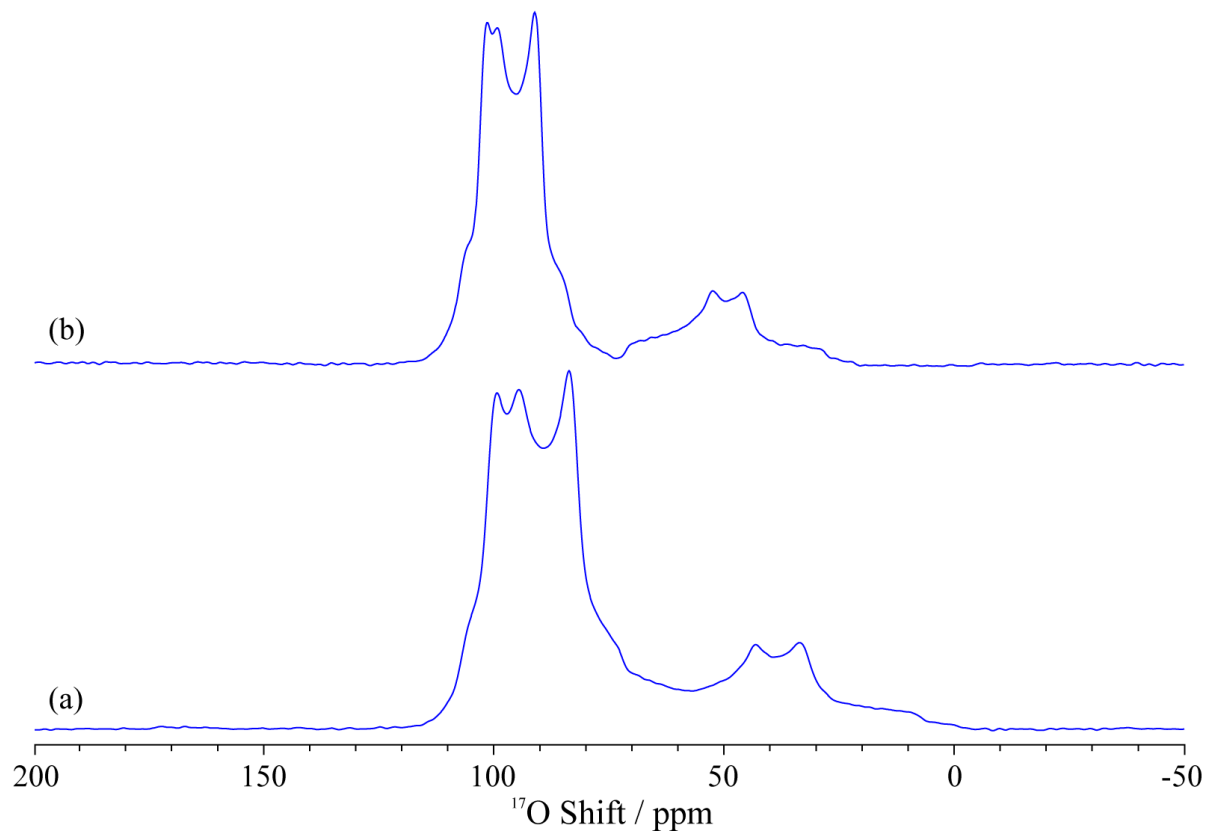


Figure S3. Room-temperature ^{17}O MAS NMR spectra of CsH_2PO_4 obtained with a MAS rate of 20 kHz at (a) 16.4 T, and (b) 20.0 T. The line narrowing of the peaks at the higher field indicates that the ^{17}O line shape is dominated by the second-order quadrupolar broadening.

5. Possible local hydrogen-bonding arrangements and their calculated NMR parameters

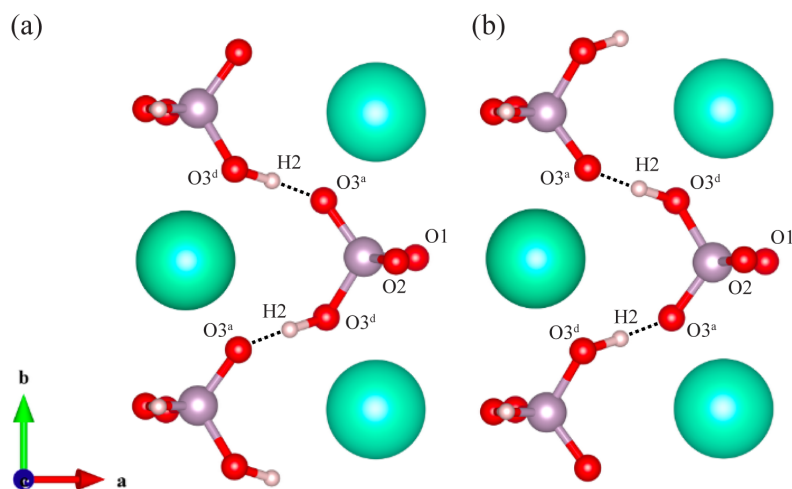


Figure S4. Possible local hydrogen-bonding arrangements based on the structure shown in Figure 1b. The calculated NMR parameters are summarized in Table S3.

Table S3. Calculated ^{17}O and ^1H NMR parameters obtained from the arrangements shown in Figure S4.

	site	$\delta_{\text{iso}}^{\text{calc}} / \text{ppm}$	$C_{\text{Q}}^{\text{calc}} / \text{MHz}$	$\eta_{\text{Q}}^{\text{calc}}$
arrangement a	O1	78.1	-6.94	0.76
	O2	110.0	-5.36	0.15
	O3	103.1	-6.61	0.77
	O3'	125.7	-5.07	0.30
	H1	11.7	-	-
	H2	13.8	-	-
arrangement b	O1	77.6	-6.90	0.80
	O2	109.6	-5.37	0.15
	O3'	125.1	-5.10	0.30
	O3	103.7	-6.60	0.76
	H1	11.5	-	-
	H2	13.9	-	-

6. Simulated 1D spectra as a function of a hopping frequency

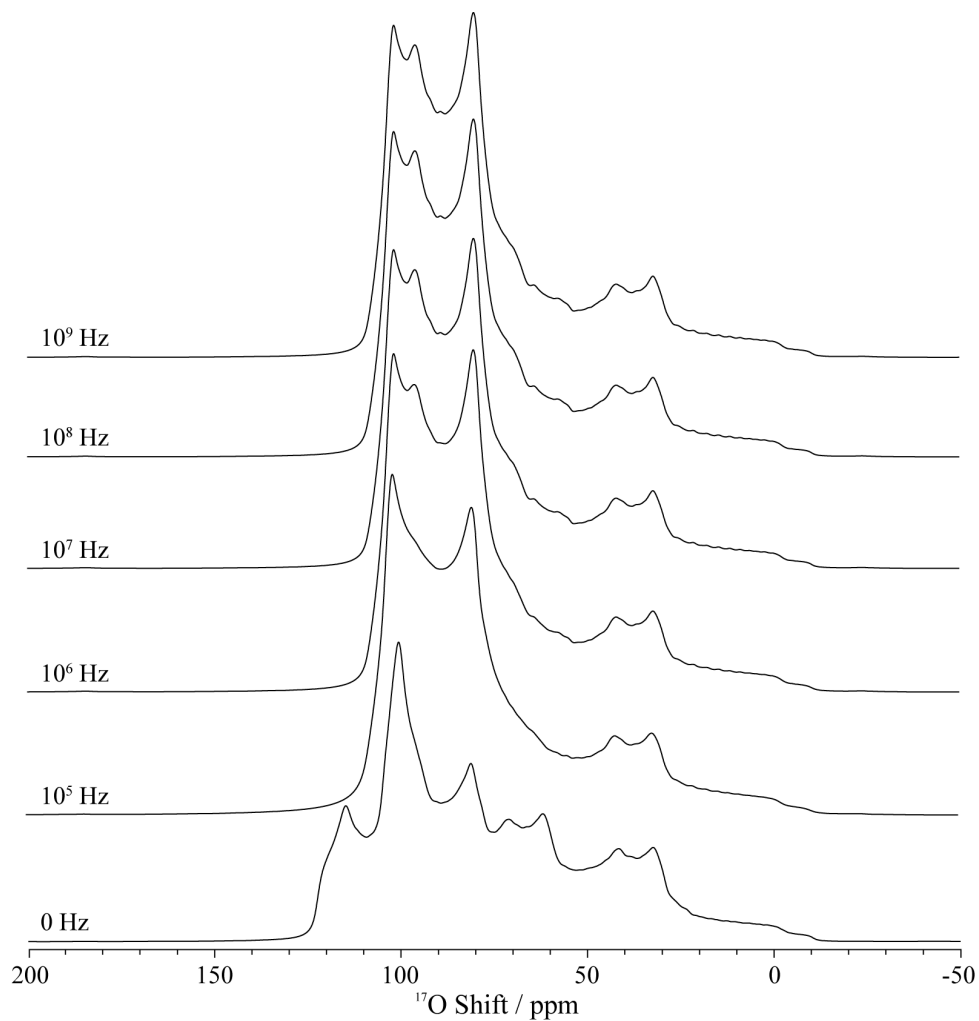


Figure S5. Simulated ^{17}O lineshapes as a function of a hopping frequency between the two H positions shown in Fig 1b and c of the main text at 16.4 T with a MAS frequency of 20 kHz. The hopping frequency was varied 0 to 10^9 Hz. The lineshape becomes essentially identical above 10^6 Hz, thus the frequency of 10^7 Hz was selected for the subsequent simulations.

7. 2D ^{17}O MQMAS spectrum.

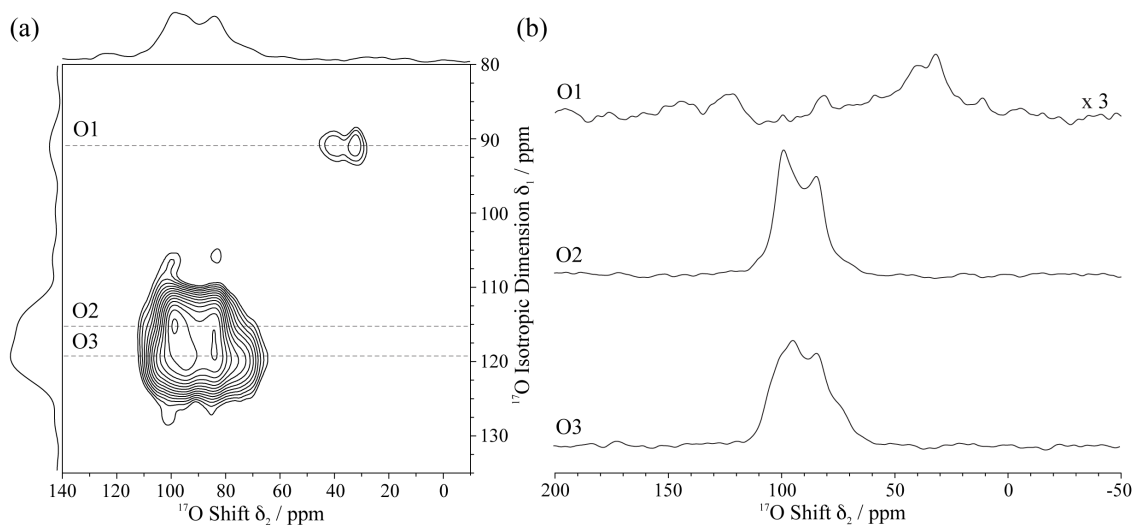


Figure S6. Room-temperature ^{17}O MQMAS spectrum of CsH_2PO_4 at 16.4 T. Sum projections are shown above and to the left of the two-dimensional spectrum. Three slices are extracted parallel to the δ_2 dimension (as indicated by the red dotted lines on the 2D spectrum) at δ_1 of ~ 90 , ~ 115 , and ~ 120 ppm, respectively. The spectrum was acquired at 16.4 T with a MAS frequency of 60 kHz, by using a typical three-pulse triple-quantum (3Q) sequence (including a z-filter),³⁻⁵ and a recycle delay of 0.1 s. 140 points were acquired on the δ_1 dimension with 9000 transients for each time increment. Optimized parameters for the MQMAS were determined directly by using the ^{17}O -enriched CsH_2PO_4 sample as a reference.

The validity of the dynamic disorder model is further confirmed by the 2D ^{17}O MQMAS³⁻⁵ NMR spectrum of CsH_2PO_4 (Figure S6a), which shows that the 1D line shape is made up of three individual components. Traces taken through each resonance parallel to δ_2 (Figure S6b) show good agreement with simulated line shapes for the O1, O2, and O3 sites assuming fast dynamic exchange (with a rate constant of $\geq 10^7$ Hz) between the two off-center structures shown in Figure 1c of the main text.

8. 2D ^1H - ^{17}O heteronuclear correlation (HETCOR) spectrum.

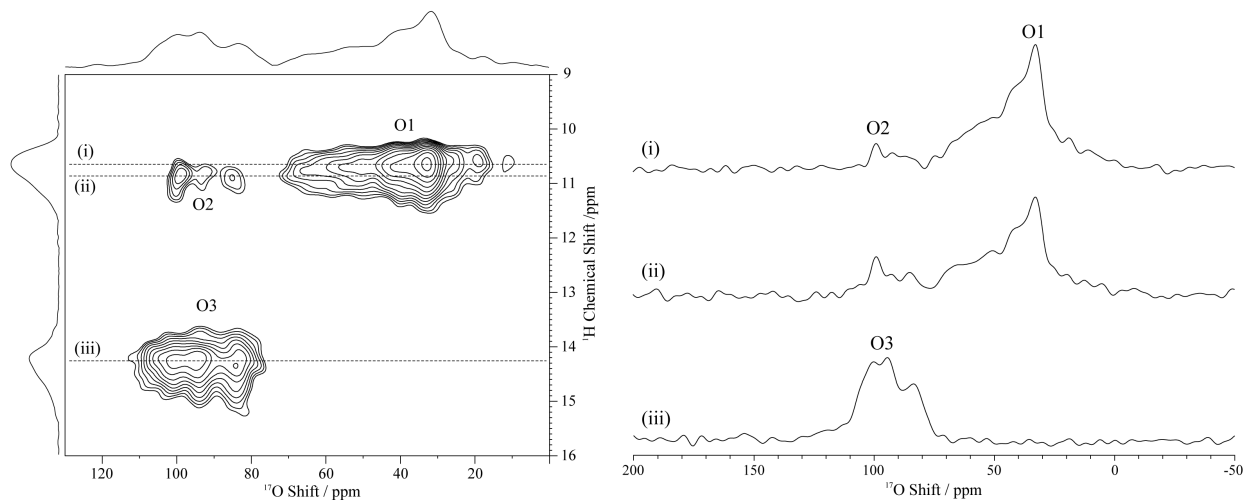


Figure S7. Room-temperature 2D ^1H - ^{17}O HETCOR spectrum of CsH_2PO_4 at 16.4 T with a MAS rate of 20 kHz and with ^1H SPINAL-64⁶ heteronuclear decoupling at a rf field amplitude of 80 – 100 kHz. RF powers of 27 kHz for ^{17}O and 100 kHz for ^1H were used. A contact time of 100 μs was used as it gave the maximum CP efficiency for the O1 site. The dotted lines in the 2D spectra indicate where each slice was taken. The correlation peaks in the 2D data show different intensities, indicating that the efficiency of a magnetization transfer varies as a function of a distance in each ^1H - ^{17}O pair and that the spatial proximity between ^1H and ^{17}O pair can be investigated.

This spectrum was obtained with a short CP contact time of 100 μs , in order to favor correlations from species in close proximity. A strong correlation centered around $\delta(^{17}\text{O}) \sim 40$ ppm, $\delta(^1\text{H}) = 10.6$ ppm corresponds to the directly-bonded O1-H1 moiety. A weaker correlation is also observed at $\delta(^{17}\text{O}) \sim 90$ ppm, $\delta(^1\text{H}) = 10.9$ ppm, corresponding to the H1 \cdots O2 hydrogen bond. A third correlation at $\delta(^{17}\text{O}) \sim 90$ ppm, $\delta(^1\text{H}) = 14.3$ ppm corresponds to the O3 \cdots H2 \cdots O3 hydrogen bond. The extracted ^{17}O traces are quite distorted and cannot be easily compared to the 1D ^{17}O

spectrum (Figure 2, main text) except for the O1 site. This is due to the fact that the CP dynamics between spin $\frac{1}{2}$ and quadrupolar nuclei are complex, the CP dynamics for different parts of the powder pattern and thus 2nd order lineshape varying noticeably.⁷

9. Variable-temperature ^{17}O MAS spectra with full spectral width.

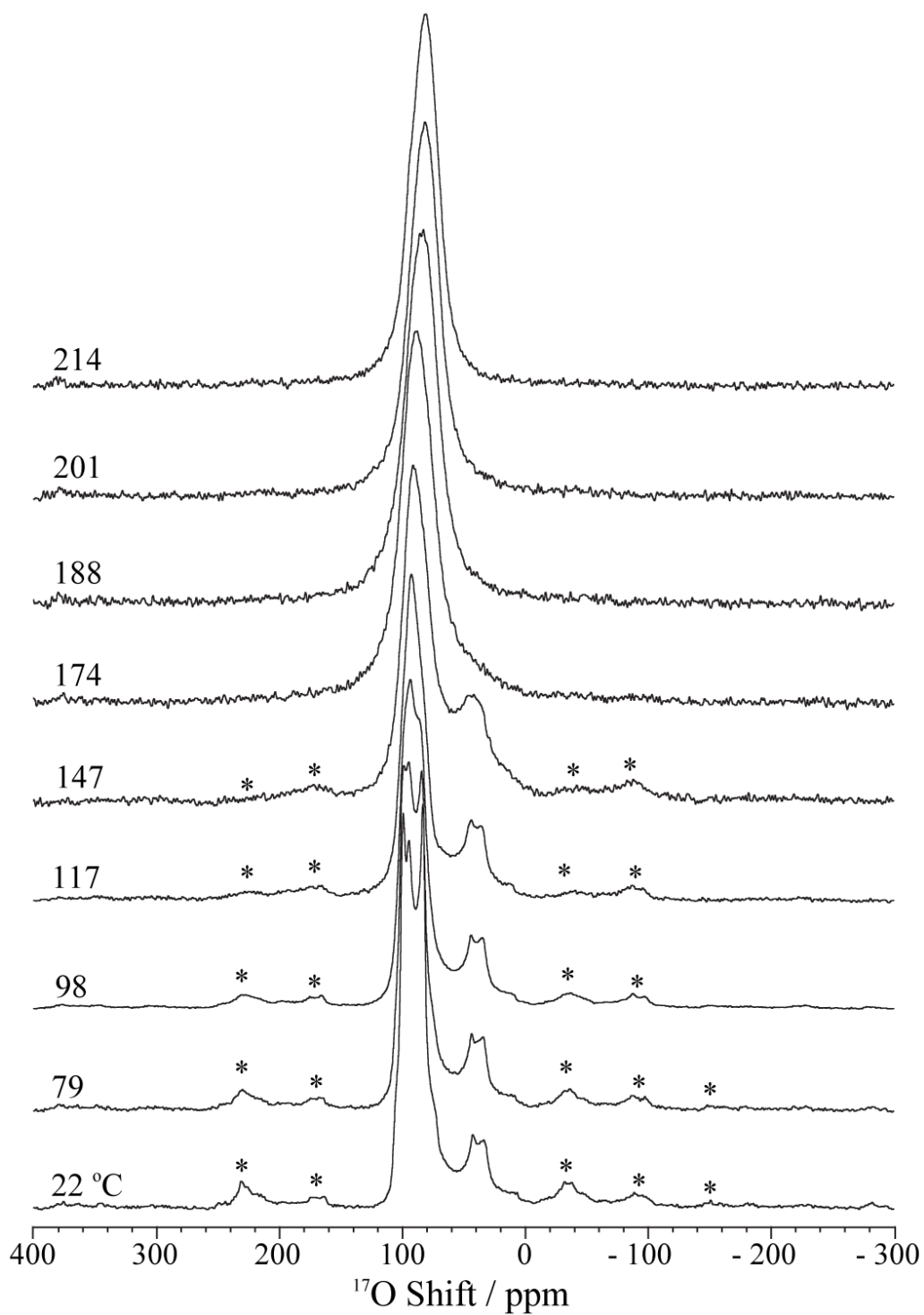


Figure S8. Variable-temperature ^{17}O NMR spectra with full spectral width at 16.4 T, with a MAS frequency of 12.5 kHz. Asterisks denote spinning side bands.

10. Room-temperature ^{17}O MAS NMR spectra with and without ^1H decoupling (Figure S9)

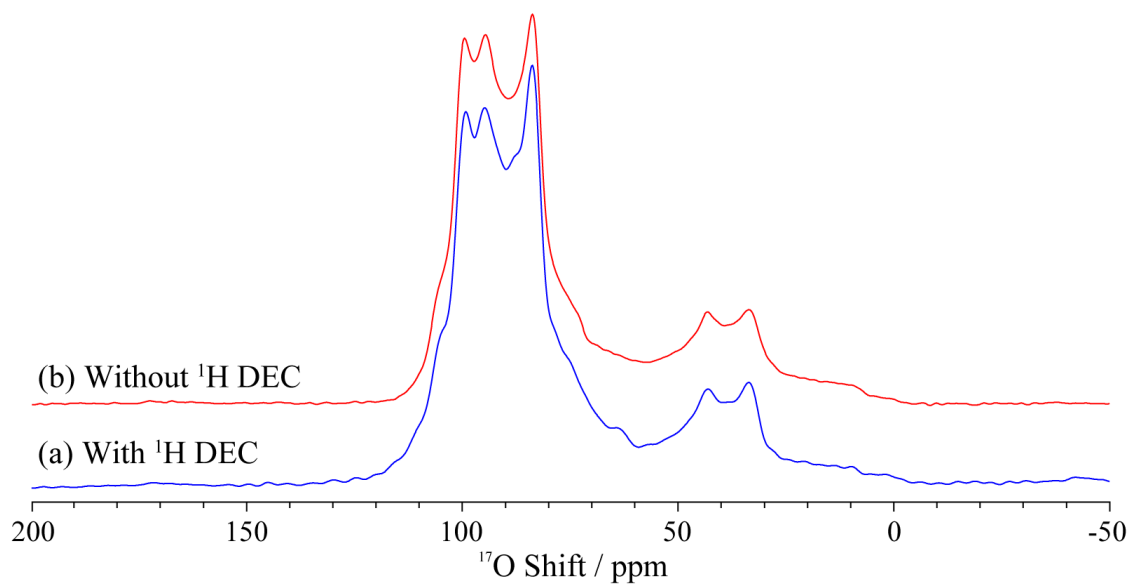


Figure S9. Room-temperature ^{17}O MAS NMR spectra of CsH_2PO_4 obtained with a MAS rate of 20 kHz at 16.4 T, (a) with and (b) without ^1H decoupling of 100 kHz.

11. Tables showing correlations between the rates of phosphate rotation and proton hop rates.

Table S4. Summary of exchange mechanism B(i), involving concerted (simultaneous) motion of all the H-atoms either directly bound or H-bonded to the oxygen atoms that move as part of the P-O rotation. The “New proton environment” represents the location and H-bonding environment of the original proton O-H or O···H species after a single (approximately 120°) rotation. Note we have only listed new proton environments for one sense of rotation; inclusion of the opposite sense of rotation does not alter the relationship between the H1-H2 exchange rate as observed by ¹H NMR and the rate of phosphate rotation.

Rotation axis (rate)	Original proton environment	New proton environment	Proton exchange event	H1-H2 exchange rate observed by NMR
P-O1 (k_2)	O3-H2	O2...H1	H2 → H1	
	O2...H1	O3...H2	H1 → H2	$2/3k_2$
	O3...H2	O3-H2	N/A	
P-O2 (k_1)	O1-H1	O3-H2	H1 → H2	
	O3-H2	O3...H2	N/A	$2/3k_1$
	O3...H2	O1-H1	H2 → H1	
P-O3 ^d (k_1)	O1-H1	O3...H2	H1 → H2	
	O3...H2	O2...H1	H2 → H1	$2/3k_1$
	O2...H1	O1-H1	N/A	
P-O3 ^a (k_1)	O1-H1	O2...H1	N/A	
	O2...H1	O3-H2	H1 → H2	$2/3k_1$
	O3-H2	O1-H1	H2 → H1	

Table S5. Summary of exchange mechanism B(ii), which involves a rotation of directly bound O-H groups and related concerted motions induced by this rotation.

Rot.	Locations		H1-H2 exchange		Concerted motion		
	Original proton environment	New proton environment	Resulting proton exchange event	H1-H2 exchange rate observed by NMR	Induced motion	H1-H2 exchange from this motion	H1-H2 exchange rate
P-O1	O3-H2	O2...H1	H2 → H1	1/3k ₂	P ⁱ -O1-H1 → O3...H2, O3-H2, or O2...H1	H1 → H2, H2, or H1	2/3k ₁
	O2...H1	O3...H2	N/A		N/A	N/A	N/A
	O3...H2	O3-H2	N/A		P ⁱⁱ -O1-H1, or P ⁱⁱ -O3-H2 → P ⁱⁱ -O3...H2	H1 or H2 → H2	1/2k ₁
P-O2	O1-H1	O3-H2	H1 → H2	2/3k ₁	N/A	N/A	N/A
	O3-H2	O3...H2	N/A		P ⁱⁱⁱ -O3-H2 → O3...H2, O1-H1, or O2...H1	H2 → H2, H1, or H1	1/3(k ₁ + k ₂)
	O3...H2	O1-H1	H1 → H2		P ^{iv} -O1-H1 or P ^{iv} -O3-H2 → P ^{iv} -O2...H1	H1 or H2 → H1	1/2k ₂
P-O3 ^d	O1-H1	O3...H2	H1 → H2	1/3k ₁	P ⁱⁱⁱ -O3-H2 → O3...H2, O1-H1, or O2...H1	H2 → H2, H1, or H1	1/3(k ₁ + k ₂)
	O3...H2	O2...H1	N/A		N/A	N/A	N/A
	O2...H1	O1-H1	N/A		P ^{iv} -O1-H1 or P ^{iv} -O3-H2 → P ^{iv} -O2...H1	H1 or H2 → H1	1/2k ₂
P-O3 ^a	O1-H1	O2...H1	N/A	2/3k ₁	P ⁱ -O1-H1 → O3...H2, O3-H2, or O2...H1	H1 → H2, H2, or H1	2/3k ₁
	O2...H1	O3-H2	H1 → H2		P ⁱⁱ -O1-H1, or P ⁱⁱ -O3-H2 → P ⁱⁱ -O3...H2	H1 or H2 → H2	1/2k ₁
	O3-H2	O1-H1	H2 → H1		N/A	N/A	N/A

References

- (1) Nelmes, R. J.; Choudhary, R. N. P. *Solid State Commun.* **1978**, *26*, 823.
- (2) Preisinger, A.; Mereiter, K.; Bronowska, W. *Mater. Sci. Forum* **1994**, *166*, 511.
- (3) Amoureux, J.-P.; Fernandez, C.; Steuernagel, S. *J. Magn. Reson., Ser. A* **1996**, *123*, 116.
- (4) Medek, A.; Harwood, J. S.; Frydman, L. *J. Am. Chem. Soc.* **1995**, *117*, 12779.
- (5) Frydman, L.; Harwood, J. S. *J. Am. Chem. Soc.* **1995**, *117*, 5367.
- (6) Fung, B. M.; Khitrin, A. K.; Ermolaev, K. *J. Magn. Reson.* **2000**, *142*, 97.
- (7) Vega, A. J. *J. Magn. Reson.* **1992**, *96*, 50.